Analytica Chimica Acta xxx (2017) 1–10

Contents lists available at ScienceDirect

Analytica Chimica Acta

journal homepage: www.elsevier.com/locate/aca

Determination of methotrexate in spiked human blood serum using multi-frequency electrochemical immittance spectroscopy and multivariate data analysis

Sereilakhena Phal [a], Britta Lindholm-Sethson [a], Paul Geladi [b], Andrey Shchukarev [a], Solomon Tesfalidet [a, *]

[a] Department of Chemistry, Umeå University, SE 90187 Umeå, Sweden
[b] Corpus Data & Image Analysis AB, Rålambsvägen 66 B, Suit 1408, SE 112 56 Stockholm, Sweden

HIGHLIGHTS

- Determination of methotrexate (MTX) in spiked blood serum using a biosensor; gold electrodes modified with antibody.
- Electrode surface modification was performed by introducing reagents while the electrodes were mounted in a flow cell.
- The electrode modification was monitored using electrochemical immittance spectroscopy and X-ray photoelectron spectroscopy.
- The method offered a wide linear working range with 8 orders of magnitude and a detection limit of 5×10^{-12} mol L^{-1}.

GRAPHICAL ABSTRACT

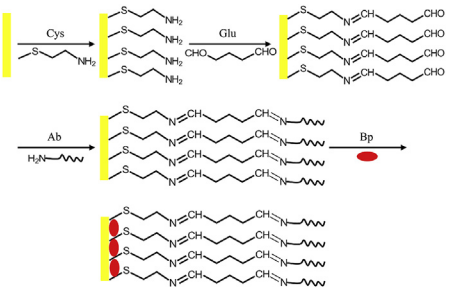

ARTICLE INFO

Article history:
Received 9 June 2017
Received in revised form
7 August 2017
Accepted 15 August 2017
Available online xxx

Keywords:
Gold electrode
Biosensor
X-ray photoelectron spectroscopy
Singular value decomposition
Multivariate calibration model
Antibody

ABSTRACT

This article describes an attempt to develop a sensor based on multi-frequency immittance spectroscopy for the determination of methotrexate (MTX) in blood serum using gold electrodes modified with antibodies. The attachment of antibodies was monitored with electrochemical immittance spectroscopy (EIS) and X-ray photoelectron spectroscopy (XPS). The EIS measurements of MTX resulted in a data matrix of size 39 × 55. The data were analysed using multivariate data analysis and showed a concentration dependence and time dependence that could be separated. This allowed the calculation of a multivariate calibration model. The model showed good linear behavior on a logarithmic scale offering a detection limit of 5×10^{-12} mol L^{-1}.

1. Introduction

Methotrexate (MTX) (Fig. 1) has been used as an efficient drug in

* Corresponding author.
E-mail address: solomon.tesfalidet@chem.umu.se (S. Tesfalidet).

http://dx.doi.org/10.1016/j.aca.2017.08.034
0003-2670/

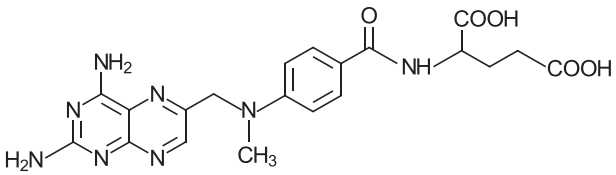

Fig. 1. Methotrexate (MTX) structure.

chemotherapy to treat a number of diseases such as rheumatoid arthritis, head and neck cancer, osteogenic sarcoma, leukemia [1,2], bladder and breast cancer [3]. However, it can also cause some side effects including lung and liver disease, low white blood cell counts [4], and could also be life threatening in case of high dose usage [5]. Therefore, monitoring the concentration of MTX in blood is necessary in order to create an optimized dosage and thereby minimize the toxicity.

Various analytical methods have been utilized for the determination of MTX including high performance liquid chromatography (HPLC) [5,6], electrospray ionization tandem mass spectrometry (ESI-MS) [7], fluorimetry [8], and capillary electrophoresis (CE) [9]. Although the demands of accuracy, selectivity, and sensitivity can be met with such methods, they demand high amount of organic solvent, complicated sample preparation and highly skilled operator, expanding the cost and the time of analysis. Owing to these considerations, sensors that are based on electrochemical methods have been proposed as sensitive, cost-effective and simple analytical tools. These include, for MTX detection, square wave voltammetry using modified electrodes [10], differential pulse voltammetry using silver solid amalgam electrode [1], differential pulse adsorptive stripping voltammetry performed on carbon nanotubes [11]. Most of the mentioned methods depend on the faradaic electrochemical behaviour of MTX at low pH and application of potential (0.2–1.2 V *vs* Ag/AgCl). Immunosensors based on electrochemical immittance spectroscopy (EIS) are an alternative type of sensors [12–19].

Recently our group reported a non-faradaic method for determination of MTX at physiological pH using electrochemical immittance spectroscopy (EIS) and multivariate data analysis [20]. In the method, the response is obtained whilst an AC is applied over a wide range of frequencies (10^5–0.5 Hz) which causes a change in the voltage-current quotient. The immittance data consists of real and imaginary parts that change slightly when MTX binds to the antibody on the electrode surface.

The complex data matrix generated from immittance measurements can be analysed by singular value decomposition (SVD), where the small changes in the immittance are highlighted. In the previous paper, some promising results were presented for trace level determination of MTX in buffer solutions [20]. In the present work, the method is further developed for analysis of MTX in human blood serum.

The electrode modification was done online with two gold electrodes mounted in a flow cell. The gold electrodes were characterized using EIS and X-ray Photoelectron Spectroscopy (XPS) that was performed before and after each modification step. Using the current method MTX could be determined at trace levels in human blood serum with a limit of detection of 5×10^{-12} mol L^{-1}

2. Experimental

2.1. Material and reagents

Gold plate electrodes (AuE) were purchased from Arrandee (Werther, Germany) and were labeled as borosilicate glass support with a dimension of 11 mm × 11 mm × 0.7 mm coated with 2.5 ± 1.5 nm chromium prior to a layer of 250 ± 50 nm gold.

Slgard® 184 silicone elastomer kit (Dow Corning, USA), comprising a silicone elastomer base and a silicone elastomer curing agent, was used for making the polydimethylsiloxane (PDMS) flow cell. The mixture of silicone elastomer and silicone elastomer curing agent (9:1, w/w) was first degassed through a vacuum chamber before pouring into a specially designed cast and allowed to harden for 24 h at room temperature.

Polyclonal sheep Immunoglobulin G (lgG) anti-methotrexate antibody (Ab) in a serum format with 0.09% sodium azide was purchased from AbD Serotec through Nordic Biosite (Täby, Sweden). Methotrexate hydrate (MTX) (≥99%, HPLC grade); cysteamine hydrochloride ($HSCH_2CH_2NH_2 \cdot HCl$), Cys (≥97%); glutaraldehyde solution ($CHO(CH_2)_3CHO$), Glu (grade II, 25% in H_2O); absolute ethanol (spectroscopy grade, 99.9%); sodium dihydrogen

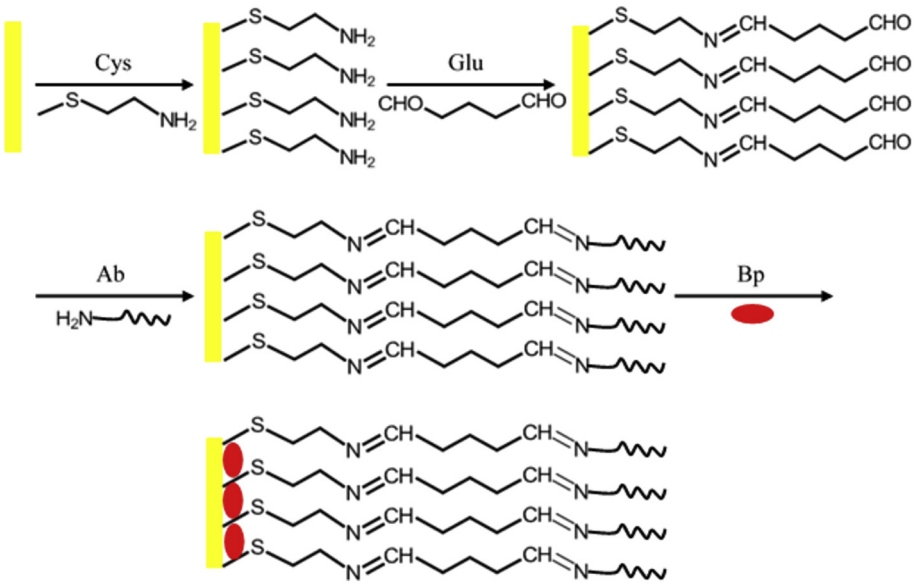

Scheme 1. Overview of the electrode surface modification steps.

Please cite this article in press as: S. Phal, et al., Determination of methotrexate in spiked human blood serum using multi-frequency electrochemical immittance spectroscopy and multivariate data analysis, Analytica Chimica Acta (2017), http://dx.doi.org/10.1016/j.aca.2017.08.034

Table 1
Experiments.

Run order	Sample	[MTX]/(mol L^{-1})
1	PBS 1	0
2	Serum (control)	0
3	PBS 2	0
4	Serum	2.73×10^{-12}
5	PBS 3	0
6	Serum	2.73×10^{-10}
7	PBS 4	0
8	Serum	2.73×10^{-8}
9	PBS 5	0
10	Serum	2.73×10^{-6}
11	PBS 6	0
12	Serum	2.73×10^{-4}
13	PBS 7	0

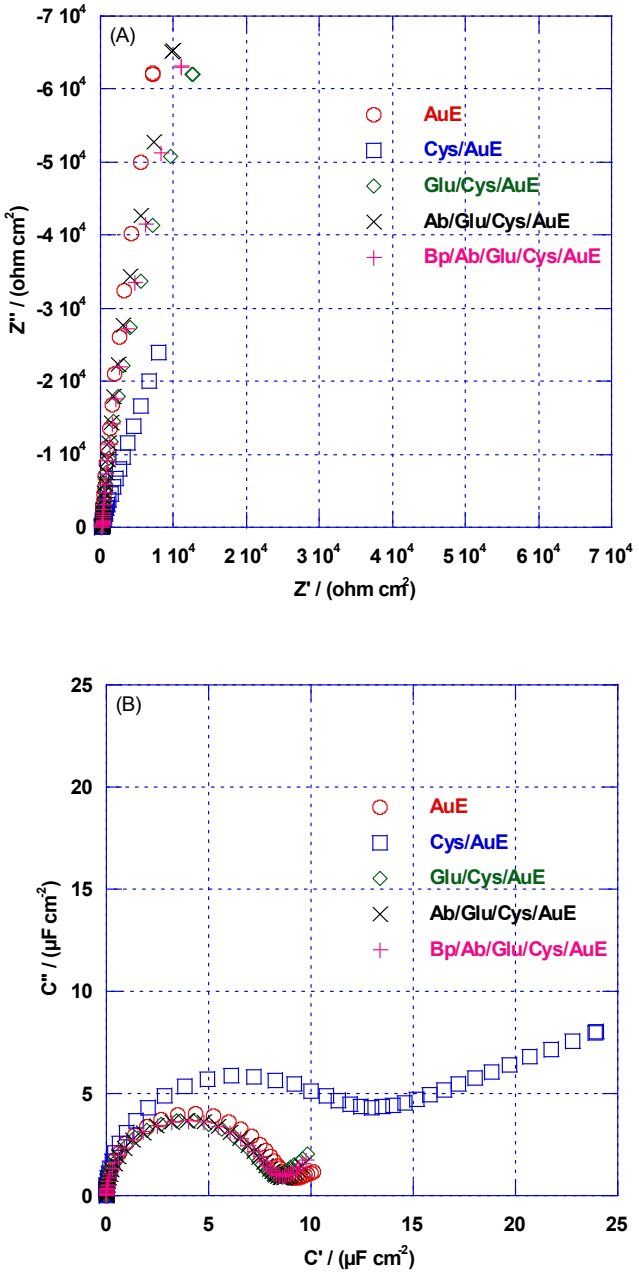

Fig. 2. Nyquist plot: (A) Complex impedance plane and (B) Complex capacitance plane for the different steps of the electrode modification.

phosphate dihydrate (NaH_2PO_4. $2H_2O$); sodium chloride and sodium hydroxide pellets were purchased from Sigma Alrich. *N*-[tris(hydroxymethyl)methyl]-acrylamide polymer (pTHMMAA) was provided from Technical Research Center (VTT, Finland). Acetonitrile (HPLC grade) was purchased from Fisher Scientific (Bishop Meadow, UK). Milli-Q water used for chemical preparation and electrode cleaning was obtained from Q-POD®'s Millipore water system.

The Phosphate buffer solution (PBS), pH 7.0, was made of 1×10^{-2} mol L^{-1} NaH_2PO_4, adjusted to the desired pH with 6.0 mol L^{-1} NaOH, and filtered.

Stock solutions of MTX were freshly prepared in PBS by weighing appropriate amount of methotrexate hydrate to give a concentration of ca 3×10^{-2} mol L^{-1}. Sodium hydroxide, 0.100 mL of 1.0 mol L^{-1}, was added in order to facilitate dissolution. Working standards of other concentrations were freshly prepared by serial dilution of the stock solution with PBS. The test solutions were degassed prior to measurement.

2.2. Instrumentation

2.2.1. Electrochemical immittance spectroscopy (EIS)

Electrochemical immittance spectroscopy (EIS) measurement was conducted with Modulab electrochemical system, ECS (Solartron Analytical, UK). A two-electrode setup was used for the EIS measurement. The electrochemical cell consisted of two modified electrodes with a PDMS flow chamber sandwiched between them [20]. The surface area of a single electrode was 7.85 mm^2 and the cell volume was 24 mm^3.

2.2.2. X-ray photoelectron spectroscopy (XPS)

The XPS spectra were collected with a Kratos Axis Ultra DLD electron spectrometer using monochromated Al K_α source operated at 150 W. Survey spectra were collected from 1100 to 0 eV at pass energy of 160 eV, and high-resolution spectra for O 1s, N 1s, C 1s, S 2p, and Au 4f were collected at pass energy of 20 eV. The surface potential was stabilized by the spectrometer charge neutralization system. The binding energy (BE) scale was referenced to the Au $4f_{7/2}$ photoelectron line, set at 84.0 eV. Processing of the spectra was accomplished with the Kratos software.

2.3. Gold electrode modification

A similar procedure as reported in a previous paper was used for modification of the gold electrodes [20]. In this work, after the cleaning step, the electrode modification was performed by injecting the reagents, with the two electrodes mounted in the flow chamber. In short:

Cleaning: Au electrodes were cleaned with a boiling solution of H_2O_2 (30%):NH_4OH (25%):H_2O (1:1:5, v/v/v) for 20 s and thereafter thoroughly washed with Milli-Q water followed by ethanol. The clean electrodes, with the PDMS flow cell sandwiched between them, were then mounted on the holder.

Attachment of cysteamine: The cysteamine solution, 0.2 mg mL^{-1} in absolute ethanol, was manually injected using a

Table 2
Graphical estimation of double layer capacitance (n = 3).

Modification steps	$C_{dl} \pm SD/(\mu F\ cm^{-2})$
AuE	8.00 ± 0.16
Cys/AuE	16.00 ± 1.36
Glu/Cys/AuE	7.32 ± 0.02
Ab/Glu/Cys/AuE	7.38 ± 0.02
Bp/Ab/Glu/Cys/AuE	7.38 ± 0.02

Please cite this article in press as: S. Phal, et al., Determination of methotrexate in spiked human blood serum using multi-frequency electrochemical immittance spectroscopy and multivariate data analysis, Analytica Chimica Acta (2017), http://dx.doi.org/10.1016/j.aca.2017.08.034

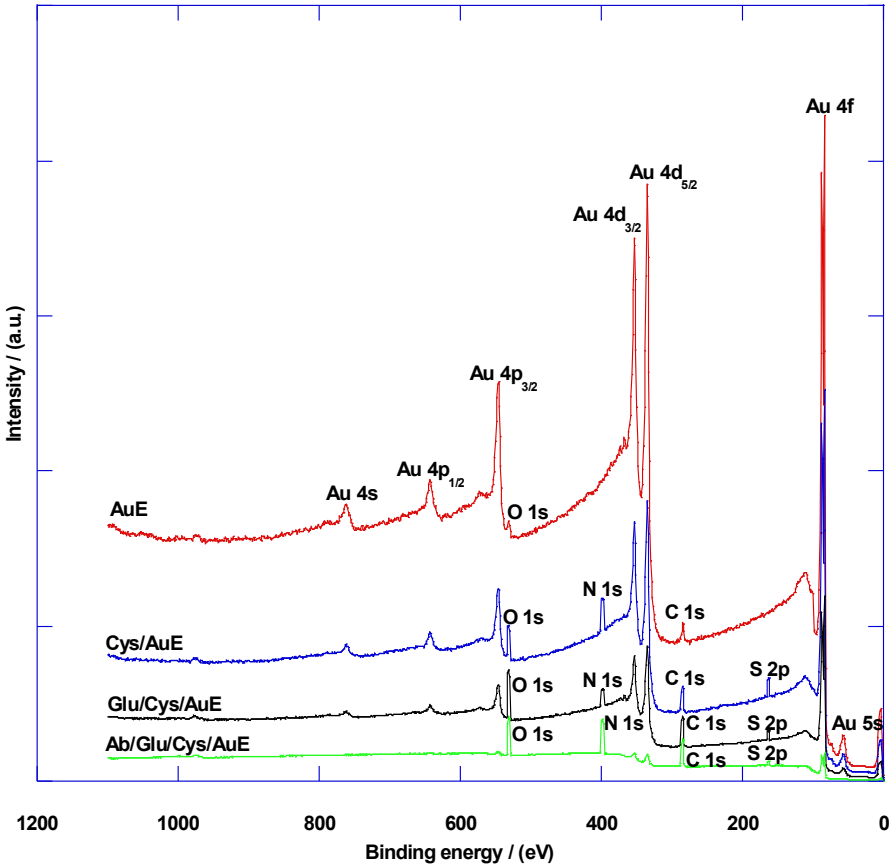

Fig. 3. Survey XPS spectra before and after the different steps of the electrode modification.

Table 3
Surface composition of gold electrode for the different steps of the electrode modification.

Electrode modification steps	Atomic concentrations, at. %				
	Au	S	C	N	O
AuE	66.7	No	26.58	No	6.72
Cys/Au	60.51	2.14	25.02	4.23	8.09
Glu/Cys/Au	55.4	1.2	28.29	3.94	11.17
Ab/Glu/Cys/Au	12.89	0.76	57.05	13.8	15.52

syringe and the flow cell was kept overnight in a refrigerator (4° C). Ethanol was flushed through the flow cell to rinse and to remove any physically adsorbed excess cysteamine from the electrode surface.

Attachment of linker: glutaraldehyde, 7.0% in PBS (v/v), used as a cross-linker, was injected into the flow cell and left to react for 20 min. Excess glutaraldehyde was flushed with Milli-Q water.

Attachment of antibody: methotrexate-antibody, 10% in PBS (v/v), 100 μL was injected and kept at 4° C overnight to allow binding to the cross-linker. The electrodes were then cleaned by flushing Milli-Q water through the flow cell.

Blocking of pinholes: *N*-[tris(hydroxyl-methyl) methyl]acrylamide (blocking polymer, Bp), 500 μg mL^{-1} in PBS, was loaded into the flow cell and kept for 20 min. The polymer blocks pinholes in the modified surface and hinders nonspecific binding [21,22]. Thereafter the flow cell was flushed with Milli-Q water.

The whole electrode modification procedure is depicted in Scheme 1.

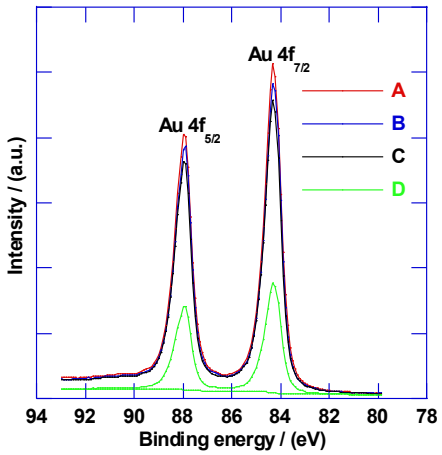

Fig. 4. XPS Au 4f spectra for AuE (A), Cys/AuE (B), Glu/Cys/AuE (C), and Ab/Glu/Cys/AuE (D).

2.4. Electrochemical immittance spectroscopy (EIS) measurement

Immittance spectra were recorded in the frequency range 10^5–0.5 Hz at 10 data points/decade with an applied alternating voltage of 10 mV. The bias DC potential between the electrodes was set to 0 V. The electrochemical cell and the peristaltic pump were put in a faradaic cage.

Please cite this article in press as: S. Phal, et al., Determination of methotrexate in spiked human blood serum using multi-frequency electrochemical immittance spectroscopy and multivariate data analysis, Analytica Chimica Acta (2017), http://dx.doi.org/10.1016/j.aca.2017.08.034

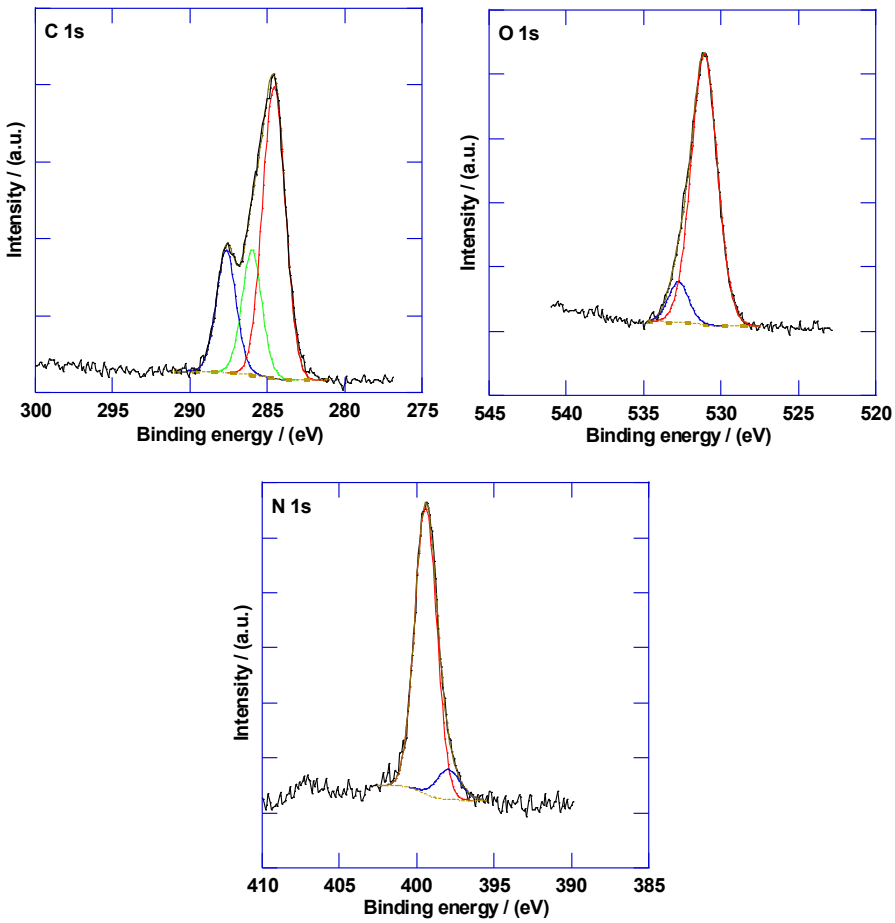

Fig. 5. XPS C1s, O 1s and N 1s spectra for the antibody modified Au electrode.

2.5. Characterization of the electrode modification steps

The gold electrodes were characterized using EIS and XPS. The immittance measurements were done on PBS before and after each modification step. Prior to measurement the PBS was pumped using a peristaltic pump, at a rate of 185 μL min^{-1}, for ca 5 min and stopped. During this step creation of bubbles was avoided.

2.6. Preparation and determination of MTX in blood serum

The human blood serum from a healthy person was obtained from the University Hospital of Umeå (NUS) and kept at −20 °C until analysis. The sample pretreatment was similar to that described by Wang et al. [10]. In short: to 1.0 mL of serum, with or without MTX spike, acetonitrile (1.5 mL) was added to remove any proteins in the serum. The serum was spiked with 0.2 mL of different concentrations of MTX. The mixture was then vortexed for 45 s and centrifuged for 10 min at 4000 rpm to discard the protein. A portion of the supernatant (2.0 mL) was withdrawn into a centrifuge tube and diluted to 15 mL with PBS. The concentration of MTX in the final solutions was 2.73×10^{-12}, 2.73×10^{-10}, 2.73×10^{-8}, 2.73×10^{-6} and 2.73×10^{-4} mol L^{-1}. The sample solutions were then degassed and stored in the dark prior to analysis with EIS on the same day. The PBS was run as blank before and after each sample with the run order shown in Table 1.

Each sample was pumped at a rate of 185 μL min^{-1} for 5.0 min to assure that the flow cell is filled with the new solution. Thereafter, the pump was stopped and five replicate EIS measurements were made for each sample, of which the last three replicates are used in the data analysis to assure that the measurements are done when the sensor is equilibrated.

2.7. Multivariate data analysis method

The immittance data are frequently displayed as:

$$\mathbf{Z} = \mathbf{Z}' + j\mathbf{Z}^{\wedge\prime\prime} \quad (1)$$

where $\mathbf{Z}$ is a total impedance, $\mathbf{Z}'$ and $\mathbf{Z}''$ are the real and imaginary parts of $\mathbf{Z}$, respectively and $j^2 = -1$, is arranged as a matrix of dimension I × K, where I is total number of measurements (39), 3 replicates for each measurement in Table 1 and K is number of frequencies in a single measurement (55) from 10^5 to 0.5 Hz.

Then, the matrix $\mathbf{Z}$ is used to generate a complex capacitance matrix:

$$\mathbf{C} = 1/[j\omega\mathbf{Z}] = \mathbf{C}' + j\mathbf{C}^{\wedge\prime\prime} \quad (2)$$

where $\mathbf{C}'$ and $\mathbf{C}''$ are real part and imaginary part of complex capacitance, involved with dielectric constants and dielectric loss, respectively. $\boldsymbol{\omega} = 2\pi\mathbf{f}$, is angular frequency (rad.s^{-1}), $\mathbf{f}$ is frequency.

For simplifying the multivariate data to obtain the data structure, singular value decomposition (SVD) is applied to the complex capacitance [23,24]. Therefore, SVD is expressed as:

$$\mathbf{C} = \mathbf{U}_i\mathbf{S}_i\mathbf{V}_i^* + \mathbf{E} \quad (3)$$

Please cite this article in press as: S. Phal, et al., Determination of methotrexate in spiked human blood serum using multi-frequency electrochemical immittance spectroscopy and multivariate data analysis, Analytica Chimica Acta (2017), http://dx.doi.org/10.1016/j.aca.2017.08.034

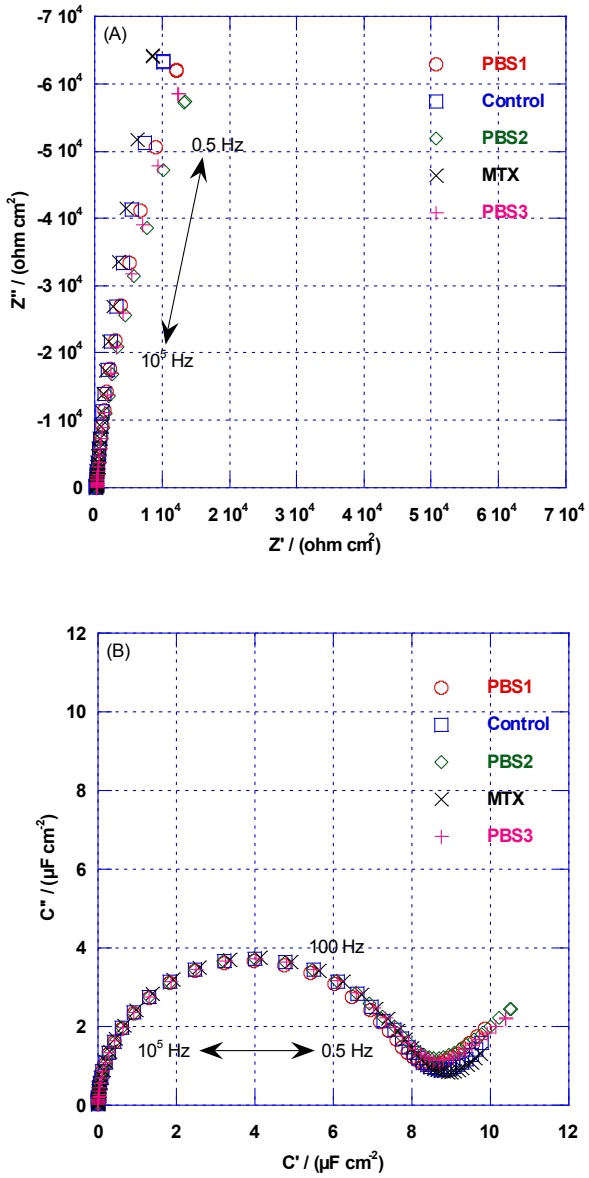

Fig. 6. Nyquist plot of (A) complex impedance and (B) Complex capacitance for PBS 1, control, PBS 2, MTX (2.73×10^{-12} mol L^{-1}) and PBS 3.

$\mathbf{U}_i$ is a unitary (complex numbers) matrix for i components, $\mathbf{V}_i^*$ is a conjugate transpose of a unitary matrix for i components.

$\mathbf{U}_i^* \mathbf{U}_i = \mathbf{I}$, $\mathbf{V}_i^* \mathbf{V}_i = \mathbf{I}$, where $\mathbf{I}$ is identity matrix

$\mathbf{S}_i$ is a diagonal matrix with real values on the diagonal for i components, $\mathbf{E}$ is a residual matrix of irrelevant data or noise which could be omitted. $\mathbf{S}_i$ is employed for the calculation of the percentage of total sum of square explained by the model, which serves as an essential diagnostic tool for selecting number of components. To find how much percentage each component explains, the squared diagonal value in $\mathbf{S}_i$ is used, the selected components are expected to have the high percentage of total sum of square in comparison to residual sum of square [24]. The total sum of square can be expressed:

$$\mathbf{SS}\text{tot} = \mathbf{S}_1^2 + \mathbf{S}_2^2 + \ldots + \mathbf{S}^2(\mathbf{E}) \quad (4)$$

where $\mathbf{S}_1$, $\mathbf{S}_2$ and $\mathbf{S}(\mathbf{E})$ are the singular value of first component, second component and residual, respectively.

The SVD data analysis was done using Matlab (The Mathworks, Inc.).

Multivariate calibration model was established to make a prediction for the MTX concentration, is indicated by:

$$\mathbf{Y} = [\mathbf{1U}]\mathbf{b} + \mathbf{f} \quad (5)$$

$\mathbf{Y}$ is the vector for the predicted MTX concentration, $\mathbf{U}$ comes from equation (3) with all values converted to real, $\mathbf{1}$ is the all-ones vector, $\mathbf{b}$ is the regression coefficients and $\mathbf{f}$ is the vector of residuals.

3. Results and discussion

3.1. Characterization using EIS

Resulting immittance spectra obtained for the different steps in the electrode modification are presented in Fig. 2.

Impedance spectra, Fig. 2A, provided capacitive lines, reflecting small changes in double layer capacitances. These differences became more clear when data was transformed into complex capacitance, which is not surprising since this transformation highlights the low frequency part of the spectra, Fig. 2B. The double layer capacitance indicates how the electrode surface is affected by the each modification step and was graphically estimated from the maximum value of the imaginary capacitance, $C_{dl} = C''_{max} \times 2$, Table 2.

The initial double layer capacitance at the bare gold electrode was increased when modified with cysteamine. This can be explained by partial protonation of the amino group in cysteamine, NH_3^+-$(CH_2)_2$-S- that has a pKa of 8.2 [25]. The coverage of the gold electrode with cysteamine is indicated by an increase in the charge storage capacity at the electrode surface due to the formation of surface-bound NH_3^+.

When glutaraldehyde (Glu) was introduced as a linker the double layer capacitance decreased. This can be explained by the increase in thickness of a layer when Glu binds to the amino group of cysteamine (Scheme 1) as shown in equation (6) [26–28].

$$C = \varepsilon_r \varepsilon_0 A/d \quad (6)$$

Here ε_0 is permittivity or dielectric constant of free space, ε_r is a relative dielectric constant of the layer, A is the electrode area and d is the layer thickness.

The remaining steps in the electrode modification, treatment with the antibody (Ab) and the blocking polymer (Bp) did not show a noticeable change in capacitance.

3.2. Characterization using XPS

X-ray photoelectron spectroscopy was used to check the effectiveness of different steps used to modify the surface of gold electrode. Corresponding survey XPS spectra (Fig. 3) provided photoelectron lines characteristic for Au, S (S 2p at 162 eV), C (C 1s at 285 eV), N (N 1s at 398 eV), and O (O 1s at 532 eV).

Atomic concentrations (at %) of different elements at the Au electrode surface before and after each modification step are reported in Table 3. Surface composition of the clean bare gold electrode (AuE) is dominated by Au, however, a significant amount of carbon and oxygen are still present, probably due to insufficient cleaning time (only 20 s) in a basic Piranha solution.

The cysteamine step resulted in appearing of additional N 1s and S 2p photoelectron lines (Fig. 3, Cys/AuE). S 2p binding energy

Please cite this article in press as: S. Phal, et al., Determination of methotrexate in spiked human blood serum using multi-frequency electrochemical immittance spectroscopy and multivariate data analysis, Analytica Chimica Acta (2017), http://dx.doi.org/10.1016/j.aca.2017.08.034

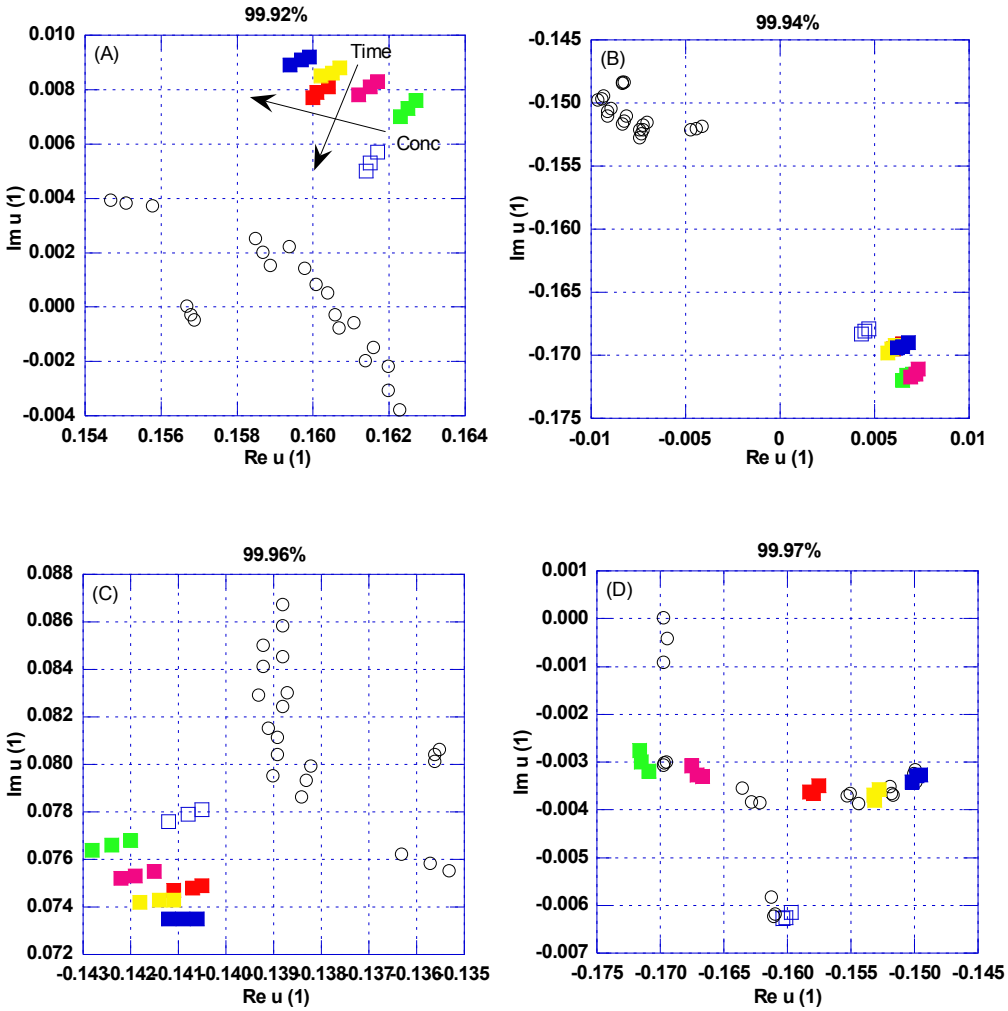

Fig. 7. The score plots of the first component of the real and imaginary score u (1) provided by SVD for (A) entire frequency regime, 55 frequencies (10^5 to 0.5 Hz), (B) 31 frequencies (10^5 to 100 Hz), (C) 25 frequencies (100–0.5 Hz) and (D) entire frequency regime using the modified electrode without antibody. Blanks (PBS, black circles), control (square unfilled blue) and MTX (green, pink, red, yellow and blue for 2.73×10^{-12}, 2.73×10^{-10}, 2.73×10^{-8}, 2.73×10^{-6} and 2.73×10^{-4} mol L^{-1}, respectively). (For interpretation of the references to colour in this figure legend, the reader is referred to the web version of this article.)

(162.1 eV) is characteristic for the Au-S chemical bond formed [29]. This together with a reasonable decrease of Au concentration indicates the attachment of cysteamine by the thiol group to the Au surface through chemisorption.

During the glutaraldehyde step (Glu/Cys/AuE) further decrease of Au and a decrease in S and N compared to Cys/AuE was observed, indicating that the Glu molecules form a top surface layer. Accordingly, the concentration of oxygen and carbon was raised because of the presence of these elements in the glutaraldehyde structure.

During the antibody-anchoring step (Ab/Glu/Cys/AuE) a significant decrease of gold and sulfur concentrations coincided with an increase in the amount of C, N, and O was observed, which is a strong evidence for the presence of antibody on the electrode surface. The antibody "layer" depresses the XPS signal of Au and S because of both elements are now much deeper in the analysed layer [30], however, the growing concentration of carbon, nitrogen, and oxygen is due to the fact that the antibody contains all these elements. Au 4f spectra (Fig. 4) demonstrate the decline in Au 4f peak intensity during the different steps in the electrode modification from (A) to (D), as it was discussed above.

To confirm the binding of antibody at the surface of gold electrode, high-resolution C 1s, N 1s, and O 1s spectra (Fig. 5) were acquired for the Ab/Glu/Cys/AuE sample. C 1s spectrum consists of three components: 284.3 eV (C-C and C-H, red), 285.8 eV (C-N, C-O green) and 287.4 eV (N-C=O, blue). The peak at 287.4 eV corresponds to the carbon in the amide function, which is typical for proteins [30]. Therefore, it is possible to assume that the antibody is present at the surface because proteins are the main constituents of the antibody.

N 1s spectrum is also typical for proteins and displays two components at 397.7 eV (blue) and 399.2 eV (red), corresponding to nitrogen in N=C [31,32] and NH_2- or –N-C=O bonds, respectively. These two types of bonding are a firm expression of a surface bound antibody.

O 1s spectrum was fitted by two components at 530.8 eV (N-C=O, red) and 532.5 eV (C-*O*-C and C-*O*-H, blue). The essential component is the bonding of O in amide group, which is characteristic for the antibody.

Please cite this article in press as: S. Phal, et al., Determination of methotrexate in spiked human blood serum using multi-frequency electrochemical immittance spectroscopy and multivariate data analysis, Analytica Chimica Acta (2017), http://dx.doi.org/10.1016/j.aca.2017.08.034

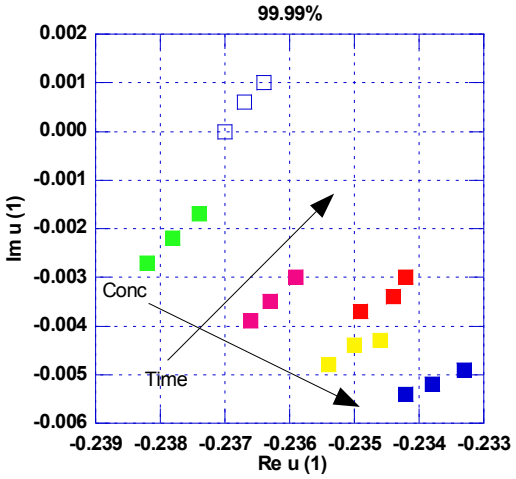

Fig. 8. The score plots of the first component of the real and imaginary score u (1) provided by SVD for the MTX concentrations and the control, 25 frequencies (100–0.5 Hz). Control (square unfilled blue) and MTX (green, pink, red, yellow and blue for 2.73×10^{-12}, 2.73×10^{-10}, 2.73×10^{-8}, 2.73×10^{-6} and 2.73×10^{-4} mol L^{-1}, respectively). (For interpretation of the references to colour in this figure legend, the reader is referred to the web version of this article.)

3.3. Multivariate data analysis of methotrexate in serum sample

The Nyquist plots of complex impedance Z″ *vs* Z′ and complex capacitance C″ *vs* C′ are displayed in Fig. 6, when the electrode was exposed to PBS, control (unspiked serum), and serum spiked with MTX to 2.73×10^{-12} mol L^{-1}. To avoid crowding, only spectra of the last replicate for the measurement in run order 1, 2, 3, 4 and 5 (Table 1) are presented.

In the impedance plane, Fig. 6A, only almost pure capacitive lines were observed, whereas in the capacitance plane Fig. 6B, subtle changes of dielectric properties were seen in the low frequency part, related to interactions on the electrode at exposure to the samples, Table 1.

The classical method of evaluating the data with equivalent circuit fitting was ruled out because of the small differences in the immittance spectra. Therefore, multivariate data analysis based on SVD was carried out to overview the entire data set, transformed to complex capacitance, as expressed in equation (2).

The experimental data formed the data matrix **C** (39 × 55) and were analyzed without any data pretreatments. The first component of real and imaginary scores u (1) explained 99.92% (%SS) of the variation (Fig. 7A). The score plot shows a grouping of the MTX scores separated from the blank and the control scores. This indicates that there is a specific recognition of the methotrexate by the antibody on the electrode surface. An additional experiment was made to further check the specificity i.e whether the separation of MTX and blank is based on the binding of MTX to the antibody or not. In this experiment the antibody was excluded from the electrode modification steps. The score plot obtained from this experiment, displayed in Fig. 7D, showed no separation between MTX and blank, indicating that the antibody that specifically binds the MTX is missing. In addition, since pTHMMAA was used to block pinholes, nonspecific binding on the electrode should also be prevented, an assumption which is supported by earlier publications [21,22,33,34].

The score plots (Fig. 7A) also indicate that there was a time drift in the response. The time drift was, however, orthogonal to the concentration dependency, both indicated with arrows, which enables to construct a calibration of the system.

Further analysis was performed by dividing the entire frequency regime (55 frequencies) into two ranges; 10^5-100 Hz (31 frequencies) and 100–0.5 Hz (25 frequencies), to find out which frequencies that are responsible for these separations. The results are displayed in Fig. 7B and C. A clear separation linked to MTX concentration was obtained when data from the low frequency range was used, which is in good accordance with what was observed in the visual inspection of the raw data in Fig. 6B. This is not surprising since binding of MTX to the antibody is expected to result in low frequency relaxations in the immittance spectra. Here, it should be noted that the concentration dependency and the time drift were still orthogonal. For the higher frequency range, the concentration dependency was lost.

Fig. 7A, B and C show a clear separation between buffer and serum solutions, the buffer is an outlier. Excluding an outlier is known to give better models of what really matters i.e, concentration. Therefore, the buffer data was excluded in the next SVD models, and only the low frequencies were used in constructing Fig. 8, where a good separation was obtained between the different concentrations and also the orthogonality between concentration and time drift was maintained.

The calibration graph for MTX (Fig. 9) was constructed based on data in Fig. 8 using equation (5), with two components, where the first and second components (u1 and u2) explained 99.99% of the variation. The linear range of the regression model was 2.73×10^{-12} to 2.73×10^{-4} mol L^{-1}. The limit of detection (LOD) was 5×10^{-12} mol L^{-1}, estimated from 3 × (SD of f), where f is the residual of the lowest concentration and SD is the standard deviation. This is the lowest limit of detection compared to previously reported methods (Table 4).

4. Conclusion

A biosensor for determination of Methotrexate in blood serum was developed. The electrode surface modification was performed in a flow system in the following order: 1) Cysteamine 2) glutaraldehyde 3) antibody 4) a pinhole blocking polymer. The different

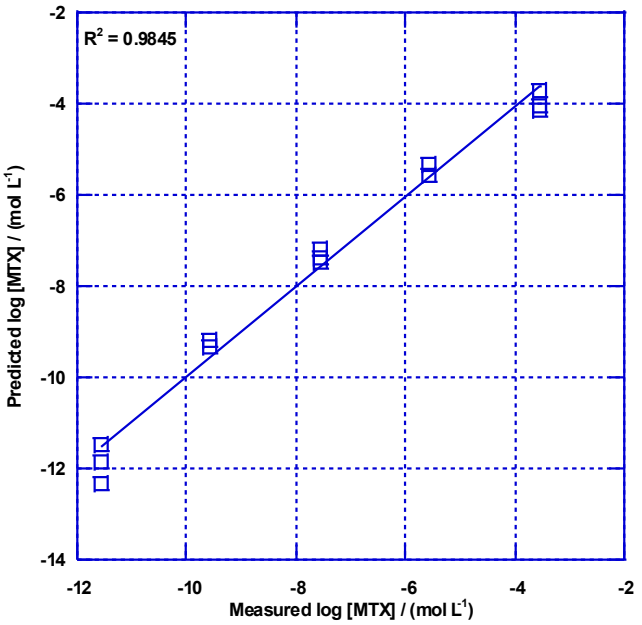

Fig. 9. Calibration curve of the predicted and measured concentration of methotrexate (273×10^{-12}, 273×10^{-10}, 273×10^{-8}, 273×10^{-6} and 2.73×10^{-10} mol L^{-1}).

Please cite this article in press as: S. Phal, et al., Determination of methotrexate in spiked human blood serum using multi-frequency electrochemical immittance spectroscopy and multivariate data analysis, Analytica Chimica Acta (2017), http://dx.doi.org/10.1016/j.aca.2017.08.034

Table 4
Comparison of electrochemical methods used for detection of MTX.

Methods	Electrode	Linear range/(mol L^{-1})	LOD/(10^{-9} mol L^{-1})	Ref
CC[a]	GCE[f]	8.0×10^{-7}–2.0×10^{-5}	350	[2]
DPV[b]	CD-GNs[g]/GCE	1.0×10^{-7}–1.0×10^{-6}	20	[35]
DPV[b]	PdAg-NG[h]/GCE	2.0×10^{-8}–2.0×10^{-4}	1.32	[36]
SWV[c]	DNA LB[i]/GCE	2.0×10^{-8}–4.0×10^{-6}	5.0	[37]
SWV[c]	DNA/SWCNT/Nafion/GCE	2.0×10^{-8}–1.5×10^{-6}	8.0	[38]
SWV[c]	Nano-Au/LC[j]/GCE	4.0×10^{-8}–2.0×10^{-6}	10	[10]
SWV[c]	PLL[k]/GCE	5.0×10^{-9}–0.2×10^{-6}	1.7	[3]
CV[d]&DPV[b]	3DC/CNTN[l]	0.7×10^{-6}–1.0×10^{-4}	70	[4]
EIS-MVA[e]	Ab/Glu/Cys/AuE	2.73×10^{-12}–2.73×10^{-4}	0.005	This work

[a] Chronocoulometry.
[b] Differential pulse voltammetry.
[c] Square wave voltammetry.
[d] Cyclic voltammetry.
[e] Electrochemical impedance spectroscopy-multivariate data analysis.
[f] Glassy carbon electrode.
[g] Cyclodextrin-graphene hybrid nanosheets.
[h] Nitrogen doped-graphene decorated with a bimetallic palladium-silver alloy.
[i] DNA Langmuir-Blodgett.
[j] L-Cysteine.
[k] Poly (L-lysine).
[l] 3D graphene-carbon nanotube network.

steps in the electrode modification were monitored with EIS; XPS with the exception of step 4. A calibration curve was prepared for MTX determination based on EIS measurements and SVD data evaluation.

The following results were obtained:

1) The binding of antibody to the electrode surface was confirmed with XPS
2) The orthogonal behavior of concentration dependence and time drift could be seen in the SVD score plot. In future experiments, an attempt should be made to get a better control or reduction of the time drift
3) The linear range of the calibration graph was 2.73×10^{-12} to 2.73×10^{-4} mol L^{-1} and the limit of detection was 5×10^{-12} mol L^{-1}
4) The frequency range 0.5–100 Hz was sufficient for good separation in the SVD plot and for making regression model. This implies the possiblility for a less expensive Immittance spectrometer for clinical use.

Future research will include a more reproducible surface preparation for the electrodes, an improved calibration model and extending the method for analysis of serum samples from patients.

Acknowledgements

The scholarship for the author from the Swedish International Development Cooperation Agency (SIDA) via the Internation Science Program (ISP) is gratefully acknowledged. This research was supported by the Objective 2 North Sweden-EU structural fond project ID 158715.

References

[1] L. Janíková-Bandžuchová, R. Šelešovská, Determination of methotrexate at a silver solid amalgam electrode by differential pulse voltammetry, Anal. Lett. 49 (2016) 122–134.
[2] L. Gao, Y. Wu, J. Liu, B. Ye, Anodic voltammetric behaviors of methotrexate at a glassy carbon electrode and its determination in spiked human urine, Electroanal. Chem. 610 (2007) 131–136.
[3] Y. Wei, L. Luo, Y. Ding, X. Si, Y. Ning, Highly sensitive determination of methotrexate at poly (l-lysine) modified electrode in the presence of sodium dodecyl benzene sulfonate, Bioelectrochemistry 98 (2014) 70–75.
[4] E. Asadian, S. Shahrokhian, A. Iraji Zad, F. Ghorbani-Bidkorbeh, Glassy carbon electrode modified with 3d graphene–carbon nanotube network for sensitive electrochemical determination of methotrexate, Sensors Actuators B Chem. 239 (2017) 617–627.
[5] I. Duran Meras, A. Espinosa Mansilla, M.J. Rodriguez Gomez, Determination of methotrexate, several pteridines, and creatinine in human urine, previous oxidation with potassium permanganate, using hplc with photometric and fluorimetric serial detection, Anal. Biochem. 346 (2005) 201–209.
[6] Y.D. Li, Y. Li, N.S. Liang, F. Yang, Z.P. Kuang, A reversed-phase high performance liquid chromatography method for quantification of methotrexate in cancer patients serum, J. Chromatogr. B Anal. Technol. Biomed. Life Sci. 1002 (2015) 107–112.
[7] A. Barbieri, L. Sabatini, P. Indiveri, R. Bonfiglioli, V. Lodi, F.S. Violante, Simultaneous determination of low levels of methotrexate and cyclophosphamide in human urine by micro liquid chromatography/electrospray ionization tandem mass spectrometry, Rapid Commun. Mass Spectrom. 20 (2006) 1889–1893.
[8] S. Chen, Z. Zhang, D. He, Y. Hu, H. Zheng, C. He, Flow-injection-electrochemical oxidation fluorimetry for determination of methotrexate, Luminescence 22 (2007) 338–342.
[9] Z. Szakacs, B. Noszal, Determination of dissociation constants of folic acid, methotrexate, and other photolabile pteridines by pressure-assisted capillary electrophoresis, Electrophoresis 27 (2006) 3399–3409.
[10] F. Wang, Y. Wang, K. Lu, X. Wei, B. Ye, Sensitive determination of methotrexate at nano-au self-assembled monolayer modified electrode, J. Electroanal. Chem. 674 (2012) 83–89.
[11] G. Oliveira, B. Janegitz, V. Zucolotto, O. Fatibello-Filho, Differential pulse adsorptive stripping voltammetric determination of methotrexate using a functionalized carbon nanotubes-modified glassy carbon electrode, Open Chem. 11 (2013).
[12] W. Limbut, P. Kanatharana, B. Mattiasson, P. Asawatreratanakul, P. Thavarungkul, A comparative study of capacitive immunosensors based on self-assembled monolayers formed from thiourea, thioctic acid, and 3-mercaptopropionic acid, Biosens. Bioelectron. 22 (2006) 233–240.
[13] S. Samanman, P. Kanatharana, W. Chotigeat, P. Deachamag, P. Thavarungkul, Highly sensitive capacitive biosensor for detecting white spot syndrome virus in shrimp pond water, J. Virol. Methods. 173 (2011) 75–84.
[14] C.I.L. Justino, A.C. Duarte, T.A.P. Rocha-Santos, Critical overview on the application of sensors and biosensors for clinical analysis, TrAC Trends Anal. Chem. 85 (2016) 36–60.
[15] C.M. Mihailescu, D. Stan, R. Iosub, C. Moldovan, M. Savin, A sensitive capacitive immunosensor for direct detection of human heart fatty acid-binding protein (h-fabp), Talanta 132 (2015) 37–43.
[16] F.C. Fernandes, A. Santos, D.C. Martins, M.S. Goes, P.R. Bueno, Comparing label free electrochemical impedimetric and capacitive biosensing architectures, Biosens. Bioelectron. 57 (2014) 96–102.
[17] F. Ricci, G. Adornetto, G. Palleschi, A review of experimental aspects of electrochemical immunosensors, Electrochimica Acta. 84 (2012) 74–83.
[18] C. Fernández-Sánchez, C.J. McNeil, K. Rawson, Electrochemical impedance spectroscopy studies of polymer degradation: application to biosensor development, TrAC Trends Anal. Chem. 24 (2005) 37–48.
[19] E.B. Bahadir, M.K. Sezginturk, Electrochemical biosensors for hormone analyses, Biosens. Bioelectron. 68 (2015) 62–71.
[20] S. Tesfalidet, P. Geladi, K. Shimizu, B. Lindholm-Sethson, Detection of methotrexate in a flow system using electrochemical impedance spectroscopy and multivariate data analysis, Anal. Chim. Acta. 914 (2016) 1–6.

Please cite this article in press as: S. Phal, et al., Determination of methotrexate in spiked human blood serum using multi-frequency electrochemical immittance spectroscopy and multivariate data analysis, Analytica Chimica Acta (2017), http://dx.doi.org/10.1016/j.aca.2017.08.034

[21] I. Vikholm-Lundin, S. Auer, A.-C. Hellgren, Detection of 3,4-methylenedioxymethamphetamine (mdma, ecstasy) by displacement of antibodies, Sensors Actuators B Chem. 156 (2011) 28–34.
[22] I. Vikholm, Self-assembly of antibody fragments and polymers onto gold for immunosensing, Sensors Actuators B Chem. 106 (2005) 311–316.
[23] P. Geladi, A. Nelson, B. Lindholm-Sethson, Complex numbers in chemometrics: examples from multivariate impedance measurements on lipid monolayers, Anal. Chim. Acta. 595 (2007) 152–159.
[24] B. Lindholm-Sethson, J. Nystrom, M. Malmsten, L. Ringstad, A. Nelson, P. Geladi, Electrochemical impedance spectroscopy in label-free biosensor applications: multivariate data analysis for an objective interpretation, Anal. Bioanal. Chem. 398 (2010) 2341–2349.
[25] Z.D. Parsons, K.S. Gates, Thiol-dependent recovery of catalytic activity from oxidized protein tyrosine phosphatases, Biochemistry 52 (2013) 6412–6423.
[26] J.S. Daniels, N. Pourmand, Label-free impedance biosensors: opportunities and challenges, Electroanalysis 19 (2007) 1239–1257.
[27] M. Darestani, H. Coster, Label-free impedance biosensing of protein/antibody interaction, in: 3rd Nanomedicine Conference, 2012.
[28] M.S. Goes, H. Rahman, J. Ryall, J.J. Davis, P.R. Bueno, A dielectric model of self-assembled monolayer interfaces by capacitive spectroscopy, Langmuir 28 (2012) 9689–9699.
[29] T.M. Willey, A.L. Vance, T. van Buuren, C. Bostedt, L.J. Terminello, C.S. Fadley, Rapid degradation of alkanethiol-based self-assembled monolayers on gold in ambient laboratory conditions, Surf. Sci. 576 (2005) 188–196.
[30] L.J. Lai, Y.W. Yang, Y.K. Lin, L.L. Huang, Y.H. Hsieh, Surface characterization of immunosensor conjugated with gold nanoparticles based on cyclic voltammetry and x-ray photoelectron spectroscopy, Colloids Surf. B Biointerfaces 68 (2009) 130–135.
[31] S. Ptasinska, A. Stypczynska, T. Nixon, N.J. Mason, D.V. Klyachko, L. Sanche, X-ray induced damage in DNA monitored by x-ray photoelectron spectroscopy, J. Chem. Phys. 129 (2008) 065102.
[32] M. Furukawa, H. Fujisawa, S. Katano, H. Ogasawara, Y. Kim, T. Komeda, A. Nilsson, M. Kawai, Geometrical characterization of pyrimidine base molecules adsorbed on Cu surfaces: Xps and nexafs studies, Surf. Sci. 532–535 (2003) 261–266.
[33] I. Vikholm-Lundin, W.M. Albers, Site-directed immobilisation of antibody fragments for detection of c-reactive protein, Biosens. Bioelectron. 21 (2006) 1141–1148.
[34] I. Vikholm-Lundin, Immunosensing based on site-directed immobilization of antibody fragments and polymers that reduce nonspecific binding, Langmuir 21 (2005) 6473–6477.
[35] Y. Guo, Y. Chen, Q. Zhao, S. Shuang, C. Dong, Electrochemical sensor for ultrasensitive determination of doxorubicin and methotrexate based on cyclodextrin-graphene hybrid nanosheets, Electroanalysis 23 (2011) 2400–2407.
[36] H. Ghadimi, B. Nasiri-Tabrizi, P.M. Nia, W.J. Basirun, R.M.A. Tehrani, F. Lorestani, Nanocomposites of nitrogen-doped graphene decorated with a palladium silver bimetallic alloy for use as a biosensor for methotrexate detection, RSC Adv. 5 (2015) 99555–99565.
[37] F. Wang, Y. Wu, J. Liu, B. Ye, DNA langmuir–blodgett modified glassy carbon electrode as voltammetric sensor for determinate of methotrexate, Electrochimica Acta. 54 (2009) 1408–1413.
[38] Y. Wang, H. Liu, F. Wang, Y. Gao, Electrochemical oxidation behavior of methotrexate at DNA/swcnt/nafion composite film-modified glassy carbon electrode, J. Solid State Electrochem. 16 (2012) 3227–3235.

Please cite this article in press as: S. Phal, et al., Determination of methotrexate in spiked human blood serum using multi-frequency electrochemical immittance spectroscopy and multivariate data analysis, Analytica Chimica Acta (2017), http://dx.doi.org/10.1016/j.aca.2017.08.034